International Journal of Bioelectromagnetism *www.ijbem.org*
Vol. 14, No. 4, pp. 204 - 210, 2012

Removal of Action Potential Influence on Local Field Potentials Using Empirical Mode Decomposition

Tatjana Loncar-Turukalo[a], Nebojsa Bozanic[a], Laszlo Negyessy[b], Fulop Baszo[b], Emmanuel Procyk[c], Dragana Bajic[a]

[a]*Faculty of Technical Sciences, University of Novi Sad, Novi Sad, Serbia*
[b]*Institute for Particle and Nuclear Physics, Wigner Research Centre for Physics, Budapest, Hungary*
[c]*Inserm U846 Stem Cell and Brain Research Institute, University of Lyon,Lyon, France*

Correspondence: T. Loncar-Turukalo, Faculty of Technical Sciences, University of Novi Sad,Trg Dositeja Obradovica 6, 21000 Novi Sad, Serbia. E-mail: turukalo@uns.ac.rs, phone:+381 69 1463 297, fax: +381 21 4752997

***Abstract.**. A method is proposed for removal of action potential bias from local field potentials in extracellular recordings with high impedance electrodes. The algorithm is based on empirical mode decomposition and provides effective removal of the spectral content which is associated with neuronal spiking. Application of the method is however not limited to this specific use, as it provides denoising solution in similar settings. The removal of artificial correlations between spikes and LFP is important for trustworthy estimation of their synchronization as disproportional influence of small set of neurons may bias activity of surrounding neuronal population.*

Keywords: Empirical Mode Decomposition, Local Field Potentials, Denoising, Action Potential, Single Unit Activity

1. Introduction

Extracellular recording is one of the most widely used techniques for studying the nervous system at the cellular level. The signal measured by an electrode placed at a neural site represents the mean extracellular field potentials (EFPs). The very first methods used low impedance microelectrodes (<1MΩ) with tips exposed a bit farther from the spike generating sources to prevent the predominance of action potentials in recorded signals. This type of electrodes can monitor the totality of the potentials in that region, consisting of dendritic events and spikes generated by several hundreds of neurons. [Logothetis, 2003;Mitzdorf,1987]. Extracellular recordings yield two signals by the means of frequency band separation. High pass filtered recording with cutoff frequency of 300 to 400Hz results in multiple-unit spiking activity (MUA). The low pass filtered recorded signal with cutoff up to 300Hz yields local field potential (LFP) which represent mostly slow events reflecting cooperative activity in neural populations.

Data obtained by high impedance electrodes (1-5 MΩ) can isolate the activity of single neurons. Single or MUA and LFP can be extracted using the same filtering procedure. Single-unit recording technique still remains the method of choice in many behavioral experiments with awake animals [Logothetis, 2003]. Relationship between the large neurons with important functions and their embedding can possibly be explained using LFP. Estimation of LFP and spiking activity from recorded signal relies on the assumption that their frequency content substantially differs. The possibility that spectral content of spiking activity waveforms spreads into LFP band, especially in single unit recordings has been overseen. There are very few studies addressing this question [Zanos et al., 2011; David et al. 2010; Galindo-Leon et al, 2010] and alerting that possible spectral contamination of LFP results in artificial correlations between spikes and LFP, manifested on many measures used for estimation of their synchronization.

It has been shown on both experimental and simulated signals [Zanos et al., 2011] that spike signatures in LFP are consequences of ineffective spectral separation, and their removal by careful preprocessing might reveal otherwise hidden relationships.

Yet the Bayesian method proposed in [Zanos et al., 2011] works on raw voltage recordings, whereas numerous LFP boards are designed to record LFPs already implementing low pass filtering (with cutoff between 150 and 300Hz). This paper proposes the method for removal of spike signatures in LFPs obtained by low pass filtering, when raw voltage recording is not available. The proposed denoising method is based on empirical mode decomposition offering adaptive removal of frequency content affected by spiking activity.

The method is tested on real experimental signals obtained from anterior cingulate cortex (ACC) in awake behaving macaque monkeys.

2. Material and Methods

2.1. Experimental procedures and task

Housing, surgical, electrophysiological, and histological procedures were carried out according to the European Community Council Directive (1986) and Départementale des Services Vétérinaires (Lyon, France). The details on surgical, experimental and task procedures are given in detail in [Quilodaron et al., 2008]. In brief two male rhesus monkeys were trained in the problem solving task (PS). Monkeys had to find by trial and error which target, presented in a set of four, was rewarded. A problem was composed of two periods: a *search* period that included all incorrect trials up to the first correct touch and a *repetition* period wherein the animal was required to repeat the correct touch several times.

Neuronal activity was recorded using epoxy-coated tungsten electrodes (1–4 MΩ at 1 kHz; FHC Inc, USA). One to four microelectrodes were placed in stainless-steel guide tubes and independently advanced into the cortex through a set of micromotors (Alpha-Omega Engineering, Israel). Recording locations were confirmed by anatomical MRI and histology [Quilodaron et al., 2008].

2.2. Extracellular recordings

Raw recordings were filtered using high pass filter (two poles Butterworth) with cutoff at 250Hz and low pass (4 poles Butterworth) with cutoff set to 3KHz for MUA and 280Hz for LFP. Neuronal activity (MUA) was sampled at 12.5 kHz and LFP at 781.25 Hz. Single unit activity was identified using online spike sorting (MSD, AlphaOmega). Since the amplitude of waveforms depends on the electrode position with respect to recorded cells, LFP data was normalized prior to analysis.

The analyzed set of data consisted of 460 pairs of LFPs and corresponding MUAs of average recording length 315s. Fig.1. presents 1s of both signals with square marks on a top panel denoting the time instants of action potentials. The activity of two neurons embedded in MUA is presented by black and grey squares. The spike signatures are clearly visible on bottom LFP waveform, as well as the presence of high frequency content. The inference on the spike position based only on LFPs is even possible using the simple threshold algorithm on the first derivative of LFPs with almost the same accuracy as this algorithm works on MUA.

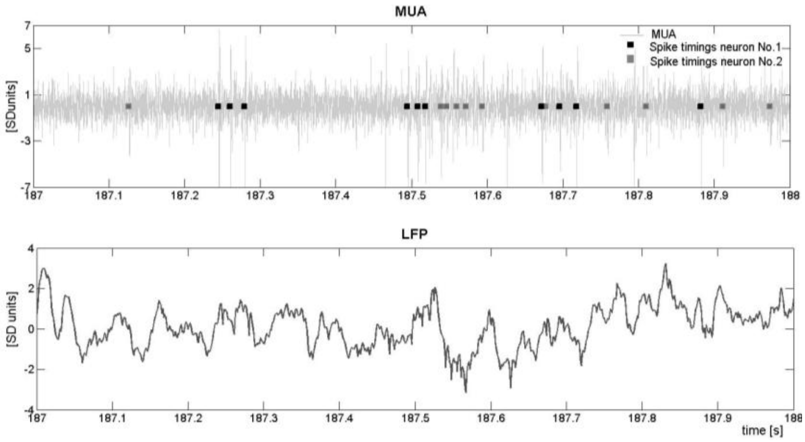

Figure 1. *MUA with annotated spike timings of two neurons (top) and corresponding LFP(bottom panel).*

To illustrate the influence of spiking activity on LFPs, Fig. 2 presents spike triggered average (STA) obtained by averaging LFP signals for each recording centered on the time of spike.

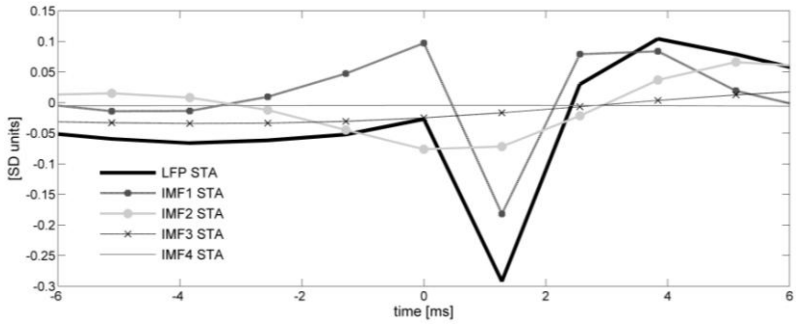

Figure 2. *Spike Trigered Average (STA)of LFP signal and its first three IMFs.*

2.3. Removing action potential influence using empirical mode decomposition

Empirical mode decomposition (EMD) is nonlinear technique developed by Huang [Huang et al., 2004] for analysis of non-stationary data by decomposition into finite number of intrinsic mode functions (*IMF*) representing zero mean AM-FM components. EMD is used in numerous practical applications and its experimental performance analysis is elaborated in [Flandrin et al., 2005;Flandrin et al. 2003], since lack of analytical formulation renders impossible theoretical analysis.

The decomposition is based on the local characteristic time scale of the data yielding *IMF*s with well behaved Hilbert transform resulting in instantaneous frequencies as functions of time. Hilbert energy spectrum is a final presentation mode providing energy-time-frequency distributions.

The details of the EMD algorithm are given in [Huang et al., 2004; Flandrin et al. 2003] here the procedure will be only briefly outlined. If *x(n)* denotes an original signal, all extrema of *x(n)* have to be identified. The upper envelope $e_{MAX}(n)$ is obtained by interpolating between maxima, and the lower envelope $e_{MIN}(n)$ comprises minima. The mean of the two envelopes *m(n)* is computed and subtracted from original signal *x(n).* The detail obtained *d(n)* follows the same procedure iteratively. The refinement of the above procedure is sifting process, which returns the detail into iteration procedure until it is zero mean, or some stopping criteria is satisfied. When the criterion is fulfilled the corresponding detail is considered the first *IMF* and the sifting process is done on the corresponding residual to obtain IMF_2.

The decomposition results in finite number K of *IMF*s and residual and allows for perfect reconstruction of the original signal:

$$x(n) = \sum_{i=1}^{K} IMF_i(n) + r(n) \tag{1}$$

where

x(n)= original signal
r(n)= residual signal
$IMF_i(n)$= the i^{th} IMF

The manipulation with modes allows selective removal of fast or slow oscillations [Flandrin et al. 2005]. The Welch estimation of power spectral density (PSD) of *IMF*s, averaged over ensemble of available LFPs reveal that the spectral content of IMF_1 and IMF_2 covers the disputable range above 100Hz, whereas the power of other *IMF*s is negligible at these frequencies, and remains below 50Hz (see Fig. 3). Another confirmation of major contribution of IMF_1 and IMF_2 to spike signatures in LFP is given in Fig. 2 where the STA for the first four *IMF*s is presented.

The proposed denoising algorithm is applied on the whole *LFP* signal selectively removing the *IMFs* whose spectral content is predominantly ($u>=70\%$) above certain, adjustable frequency f_{MAX}. The selection of f_{MAX} should cover α, β, and low γ band and partially high γ band [65-140Hz]. The explanation for partial coverage of high γ band can be found by closer inspection of the spectral content of the action potential waveform. Namely, PSD of action potential is dominated by *HF* (around 1-2kHz), but an enlargement at *LF* band reveals a certain amount of power particularly at (90-200Hz) [Zanos et al., 2011]. Unfortunately these frequencies are often examined in LFP studies.

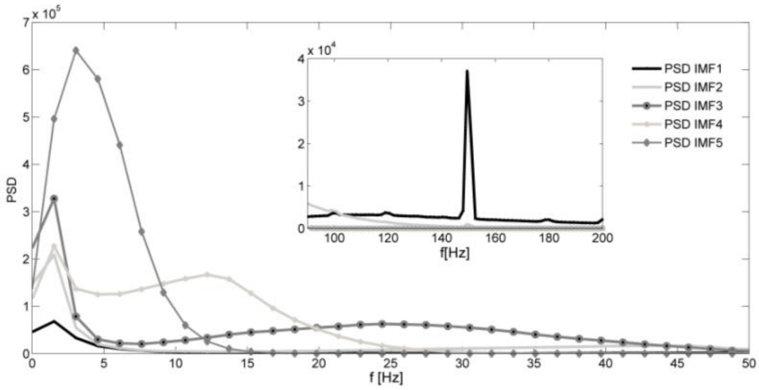

Figure 3. *Power Spectral Density (PSD) of the first five IMFs enlarged for [0-50Hz] and inset figure for [90-200Hz]*

Another argument for possible removal of *IMF*s with the spectral content above f_{MAX} is the contribution of *IMFs* to *LFP*, based on empirically observed energies of *IMFs*. The energy E_{IMF} is estimated as:

$$E_{IMF}[i] = \sum_{n=1}^{N} IMF_i^2(n) \qquad i = 1,..K \tag{2}$$

where

IMF$_i$(n) = the ith IMF

E$_{IMF}$(i) = estimated energy of the ith IMF.

The obtained energies with 95% confidence intervals (see Fig.4) indicate that IMF_1 and IMF_2 have significantly lower energies then modes IMF_4 to IMF_8.

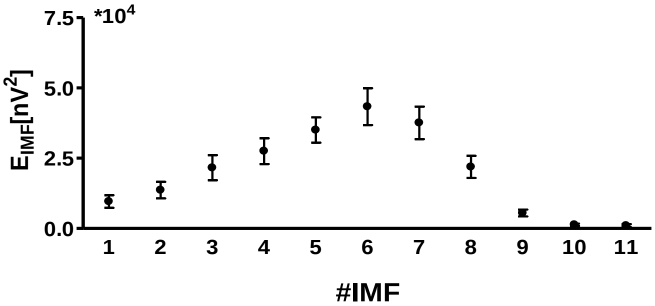

Figure 4. *The estimated energies of 11 IMFs and 95% confidence intervals*

The proposed algorithm removes the disputable frequency content performing EMD decomposition by the rule on IMF_1, IMF_2, IMF_3 and residual. The procedure starts from the whole *LFP(n), n=1,…N*. The depth of iteration procedure is denoted with *j*, *j=0* for IMFs of original signal. The algorithm starts with the parameters initialization, and counters setting *i=1;j=0*.

1. Decomposing the signal using EMD to get the first three *IMFs* and residual. The *IMFs* are processed starting from the first *IMF* at the level *j*, IMF_i^j .
2. PSD estimation of IMF_i^j .

   case 1.

   If the percentage of power for frequencies $f>f_{MAX}$ is beyond separation bound *u*%, the IMF_i^j is removed from the signal; *i=i+1*, back to step 2 (proceeding with the IMF_{i+1}^j)

   case 2

   If the power is partially *(> l%)* above f_{MAX}, IMF_i^j is further decomposed into subIMFs to remove disputable content, preserving the most of its power bellow separation bound. Move to step 3.

   case 3

   If the power of IMF_i^j is (*100-l*)% below f_{MAX}, algorithm moves to the upper iteration level *j-1*, and proceeds with the following *IMF* at that level. If j=0; *END*, otherwise back to step 1. $i=i+1; j=j-1$;

3. The *IMF* decomposition is realizable using the following manipulation. From the critical *IMF* new signal $dIMF_i^j$ of the first differences is created, $\Delta_k = IMF_i^j(k+1) - IMF_i^j(k)$, including the first *IMF* sample to enable perfect reconstruction

$$dIMF_i^j = [IMF_i^j(1) \quad \Delta_1 \quad \Delta_2 \quad \dots \Delta_{N-1}] \tag{3}$$

where

$dIMF_i^j$ = signal of the first differences of IMF_i^j

$\Delta_k = IMF_i^j(k+1) - IMF_i^j(k)$

dIMF is decomposable using EMD. After decomposition, along derived *IMF*s and residual *r* the cumulative sum is calculated yielding *cIMFs* and *cr*. It is easy to verify that the discrete integration procedure enables perfect reconstruction of the IMF_i^j from *cIMF*s and *cr* using Eq.1.

The $cIMF_1^j$ becomes the new signal which iterates from the step 1, $j=j+1$; $i=1$;

The iteration is stopped at depth *j* when the IMF_1^j fulfills the criteria for removal, or when the certain depth (set to $j=6$) is reached consequently removing the IMF_1^j produced at that level. The stepwise return to level j=0 effectively follows. The denoised signal is obtained using Eq.(1) from corrected *IMF*s for $j=0$ and residual.

Using the proposed method removal of the entire *IMF*s for $j=0$ is avoided, thus minimizing the distortion of original LFP signal reducing it to unavoidable level. The algorithm parameters u, l, f_{MAX} are adjustable to suit the needs of different experimental settings and signal to noise ratios.

The rule of EMD decomposition into IMF_1 and residual can as well be applied. It simplifies the procedure and implementation.

3. Results

The performance of the algorithm is evaluated on the ensemble of available experimentally recorded LFPs. The adjustable parameters were set to f_{MAX}=90Hz, u=70%, *l*=5%, to suit particular need. The algorithm was first tested on simulated signals (triangular wave with added noise with uniform distribution but with different amplitude levels), to assess the effect produced to original signal. By changing the parameters, a great portion of added noise could be eliminated, revealing the original waveform masked by added noise.

Despite the significant length of LFP recordings, the algorithm works reasonably fast (even when applied in Matlab), with EMD of the whole signal being the most time consumable task. Thus, EMD was limited to 10 iterations in sifting process, and the number of decomposition modes can be set to one (faster option), or three (as presented).

The procedure in average ended at level *j*=4 for IMF_1, and at level *j*=2 for IMF_2, whereas from IMF_3 the PSD condition was always satisfied (as observable from Fig. 3). The performance of algorithm on PSD of *IMF*s is presented in Fig. 5. Panel a) represents the enlarged detail of interest where PSD of *IMF*1 is presented before iteration procedure and after. It is obvious that the proposed algorithm minimizes the frequency content above the set limit, which here eliminates the need to use notch filter to remove the line noise harmonics at 100 and 150Hz. Panel 2 presents the same for IMF_2, the removed portion of the spectra is here clearly visible, and the power bellow 50Hz is mainly preserved. At this point it should again be emphasized that the contribution of IMF_1 and IMF_2 to overall LFP power at frequencies bellow 90Hz is almost negligible (PSD (IMF_6) and further were left out on purpose in Fig. 3 as they would mask the contributions from $IMF_{1\text{-}4}$ at these frequencies).

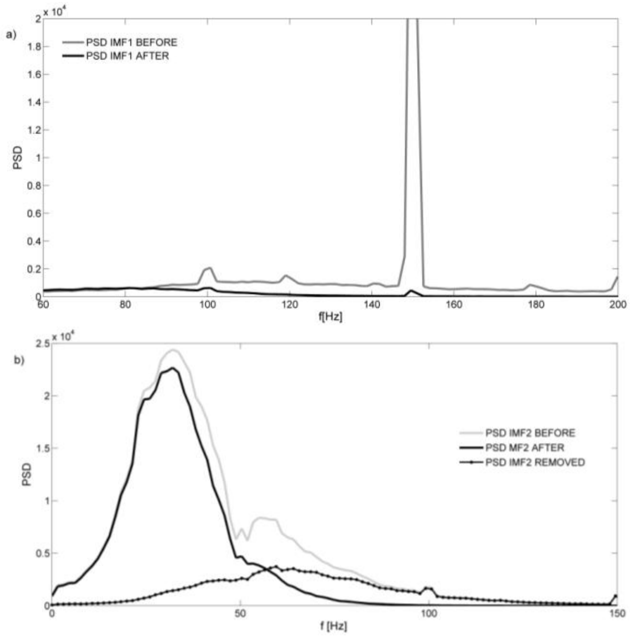

Figure 5. *The spectral content of a)IMF$_1$ and b) IMF$_2$ before and after proposed denoising*

The gross effect of algorithm's implementation is clearly visible in Fig.6 on STA, one of the most popular metrics of LFP-spike synchronization. The results obtained by our algorithm are comparable to those obtained in [Zanos et al., 2011; David et al., 2010] while exerting minimal influence on LFP signal. The expected effect was as well noted on spike field coherence, SFC, measure of spike LFP synchronization at different frequencies. It is obtained as LFP STA power spectra divided pointwise with the average power spectra of LFP segments included in STA analysis. After algorithm implementation the dominating SFC at higher frequencies disappears.

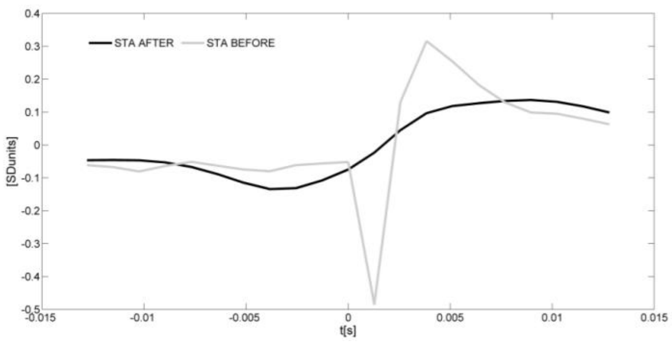

Figure 6. *STA before and after removal of frequency content above f_{MAX}*

4. Conclusions

The paper presents the method for removing the influence of action potential waveform on local field potentials in high impedance electrode recordings. The method based on recursive EMD procedure removes the frequency content above specified frequency level minimally distorting the LFP band of interest. The novelty proposed within the algorithm is the *IMF* manipulation to enable its further decomposition.

The method is suited for LFP signals already filtered in the acquisition process. It eliminates the need for further LFP filtering to remove power line harmonics and undesirable HF content produced by action potentials. The effect on STA and SFC clearly presents the effectiveness of the approach.

Future work is possible in extending the procedure on LFP extraction from raw extracellular recordings, which is now possible by LF filtering (mostly spread, but obviously not effective method for separation), by subtraction of the mean spike waveform in duration of 3ms (1ms before spike and 2ms after), by using linear interpolation of raw signal in the same interval around spike, and by the Bayesian method proposed in [Zanos et al.2011].

Acknowledgements

This research is funded in part by grants TR32040 and III41013, Serbian Ministry of Science and Technological Development and by grant 114-451-2061/2011-01, Provincial Secretariat for Science and Technological Development of Autonomous Province of Vojvodina, Republic of Serbia.

References

David SV, Malaval N, Shamma SA. Decoupling action potential bias from cortical local field potentials. *Computational Intelligence and Neuroscience*, 2010: 393019, 2010.

Flandrin P, Gonclaves P, Rilling G. On Empirical mode decomposition and its algorithms. In proceedings of the IEEE-EURASIP Workshop on Nonlinear Signal and Image Processing NSIP03,Grado (I), 2003.

Flandrin P, Gonclaves P, Rilling G. EMD equivalent filter banks: from interpretation to applications. In Hilbert-Huang Transform and its Applications. Huang NE and Shen SS, Editors. World Scientific, Singapoure, 2005, 57-74,

Galindo-Leon EE, Liu RC. Predicting stimulus-locked single unit spiking from cortical local field potentials. *Journal of Computational Neuroscience*, 29: 581-597, 2010.

Huang NE, Shen Z, Long SR. The empirical mode decomposition and Hilbert spectrum for nonlinear and non-stationary time series analysis. *IEEE Signal Processing Letters*, 11(2):112-114,2004.

Logothetis NK. The Underpinnings of the BOLD Functional Magnetic Resonance Imaging.*The Journal of Neuroscience,* 23(10):3963-3971, 2003.

Mitzdorf U. Properties of the evoked potential generators: current source density analysis of visually evoked potentials in the cat cortex. *International Journal of Neuroscience*, 33(1): 33-59, 1987.

Quilodran R, Rothé M, Procyk E. Behavioral Shifts and Action Valuation in the Anterior Cingulate Cortex. *Neuron*, 57:314-325, 2008.

Zanos TP, Mineault PJ, Prack CC. Removal of spourius correlations between spikes and local field potentials. *Journal of Neurophysiology*, 105:474-486, 2011